Immunology
The Journal of cells, molecules, systems and technologies

British Society for immunology

IMMUNOLOGY ORIGINAL ARTICLE

Efficiency of T-cell costimulation by CD80 and CD86 cross-linking correlates with calcium entry

Markus Thiel,[1,*] Melodie-Jo Wolfs,[2,*] Stefan Bauer,[1] Anna S. Wenning,[2] Tanja Burckhart,[1] Eva C. Schwarz,[2] Andrew M. Scott,[3] Christoph Renner[1,*] and Markus Hoth[2,*]

[1]*Klinik und Poliklinik für Onkologie, Universitäts-Spital Zürich, Zürich, Switzerland,* [2]*Department of Biophysics, Saarland University, Homburg, Germany, and* [3]*Ludwig Institute for Cancer Research, Austin Hospital, Melbourne, Australia*

doi:10.1111/j.1365-2567.2009.03155.x
Received 20 February 2009; revised 15 April 2009; accepted 29 June 2009.
*These authors contributed equally.
Correspondence: M. Hoth, Department of Biophysics, Saarland University, Kirrberger Strasse 58, 66421 Homburg, Germany.
Email: markus.hoth@uks.eu
Senior author: Markus Hoth

Summary

Costimulation is a fundamental principle of T-cell activation. In addition to T-cell receptor engagement, the interaction between CD80 and/or CD86 with CD28 and/or cytotoxic T-lymphocyte antigen 4 (CTLA-4) receptors is required to regulate T-cell activation and tolerance. While the importance of costimulation is clearly established, the exact molecular mechanism is unknown. We demonstrate that T-cell proliferation and the ability of $CD8^+$ T-effector cells to kill were enhanced slightly by CD80 but dramatically by CD86 costimulation. To further analyse the cellular process of costimulation, we developed a single-cell assay to analyse Ca^{2+} signals following costimulation with bi-specific antibodies. We found that this stimulation method worked in every human T-cell that was analysed, making it one of the most efficient T-cell activation methods to date for primary human T cells. The enhanced proliferation and killing by costimulation was paralleled by an increase of Ca^{2+} influx following CD86 costimulation and it was dependent on CD28/CTLA-4 expression. The enhanced Ca^{2+} influx following CD86 costimulation was abrogated by an antibody that interfered with CD28 function. The differences in Ca^{2+} influx between CD80 and CD86 costimulation were not dependent on the depletion of Ca^{2+} stores but were eliminated by the application of 10 μM 2-aminoethyldiphenyl borate which has recently been shown to enhance stromal interaction molecule 2 (STIM2)-dependent Ca^{2+} entry while reducing STIM1-dependent Ca^{2+} entry. Our data indicate that differences in the efficiency of costimulation are linked to differences in Ca^{2+} entry.

Keywords: calcium channel; calcium release-activated Ca^{2+} channel; lymphocyte; ORAI channel

Introduction

The T cells represent the cornerstone of the cellular human immune system and when adequately activated can eliminate virus-infected or even malignantly transformed cells very efficiently. The activation process of resting T cells to become potent effector cells is complex and requires multiple receptor–ligand interactions. Activation of T cells is initiated through the interaction of T cells and antigen-presenting cells. The specificity of this response is determined by the binding of the T-cell receptor (TCR) to peptide–major histocompatibility complex (MHC) complexes displayed on the surface of antigen-presenting cells.[1,2] This specific protein–protein interaction needs at least 10 seconds to trigger TCR-dependent intracellular signalling pathways.[3] To produce an effective TCR response, an additional interaction of the CD4 or CD8 co-receptors with invariant parts of the MHC–peptide complex is required to stabilize the TCR-agonist peptide–MHC complex.

Upon TCR activation, the Src kinases Fyn and Lck phosphorylate the tyrosine residues in their immune-receptor tyrosine-based activation motifs (ITAMs), which allow activation of the ζ-chain-associated protein of molecular weight 70 000 (ZAP-70).[4,5] ZAP-70 phosphorylates the adaptor proteins LAT and SLP76, which activate phospholipase Cγ (PLCγ) through the Src-like tyrosine kinase Tec.[3] The PLCγ cleaves phosphatidylinositol 4,5 bisphosphate and generates the second messengers inositol 1,4,5,-trisphosphate ($InsP_3$) and diacylglycerol.[5–8] The $InsP_3$ binds to the $InsP_3$ receptor in the membrane of the endoplasmic reticulum, which is the main Ca^{2+} store, and

initiates the release of its stored Ca^{2+}.[6–9] Depletion of Ca^{2+} from the endoplasmic reticulum induces stromal interaction molecule (STIM1)-dependent activation of store-operated calcium release-activated Ca^{2+} (CRAC) channels in the plasma membrane.[6–11] ORAI (also called CRACM) proteins have been shown to form the pore of the CRAC channel complex.[12–15] STIM1 has been shown to activate CRAC/ORAI channels.[16–18] The function of its close relative STIM2 is not as well understood.[19–21] Analysis of STIM1- and STIM2-deficient mouse T cells revealed that they are both important for Ca^{2+} influx, T-cell activation and the development and function of regulatory T cells, with STIM2 being less important than STIM1.[22] Parvez *et al.* [21] demonstrated that STIM2 activates CRAC channels but that this activation is much more complicated because it involves store-dependent and store-independent processes. Influx of Ca^{2+} through STIM-activated CRAC/ORAI channels elevates the intracellular calcium concentration $[Ca^{2+}]_i$ in T cells for times lasting from minutes up to hours.[23]

A rise of $[Ca^{2+}]_i$ as the result of Ca^{2+} release and Ca^{2+} influx through store-operated CRAC channels is critically involved in the regulation of the three most important transcription factor families controlling transcriptional activity and T-cell proliferation.[5,9,24,25] It is remarkable that 75% of all activation-regulated genes are dependent on Ca^{2+} influx through the plasma membrane via CRAC channels.[26] Decreasing $[Ca^{2+}]_i$ leads to inhibition or reduction of T-cell activation and proliferation,[23,27–29] highlighting the great influence of $[Ca^{2+}]_i$ on T-cell-based immune responses.

While TCR stimulation alone activates many signalling cascades, including Ca^{2+} signalling, it is not sufficient for optimal T-cell activation in most circumstances and a costimulatory signal is required for adequate activation. In primary T-cell responses, CD28 is the best known positive costimulator of T-cell activation, whereas cytotoxic T-lymphocyte antigen 4 (CTLA-4; CD152) provides an inhibitory signal.[30,31] Despite their structural homology, CTLA-4 and CD28 are fundamentally different with respect to their effects on T-cell activation. Both molecules share the same ligands [CD80 (B7-1) and CD86 (B7-2)] expressed on antigen-presenting cells or target cells, with the distinction that CTLA-4 binds to both with a higher affinity.[32–34] It was demonstrated that CD80 is the preferred ligand for CTLA-4, whereas CD86 is preferred by CD28.[35–37] The localization and expression patterns of these two molecules also differ. CD28 is constitutively expressed on the cell surface of naïve and activated T cells, whereas CTLA-4 is not detectable on naïve T cells and is induced only upon T-cell activation.[37,38] Once expressed, CTLA-4 localizes to an endosomal compartment because it contains a tyrosine-based intracellular localization motif in its cytoplasmic tail.

Our group has focused on the concept of T-cell activation by mimicking the physiological 'two-signal' model[39] in recent years. We developed bi-specific molecules that cross-link human T cells to antigen-positive target cells bypassing MHC restriction. Signal one is delivered by an anti-CD3 antibody of moderate activity that can be significantly enhanced by the addition of costimulatory molecules delivering signal two. To identify the most appropriate costimulatory molecule in this setting, extracellular domains of CD80 and CD86 were linked to antigen-specific single-chain fragment variable antibodies (scFv) and their potential to mediate T-cell proliferation and cytotoxicity were tested. Here we demonstrate that this activation method can virtually activate every single T cell and we can 'tune' the activation response through the costimulatory molecules used. Interestingly, we can correlate the difference in the efficiencies of T-cell activation induced by CD80 or CD86 cross-linking with Ca^{2+} influx. In addition, our data point to an important role of STIM2 for T-cell activation following formation of the immunological synapse after costimulation.

Materials and methods

Cell lines, reagents and vectors

RPMI-1640 [supplemented with 10% (volume/volume) heat-inactivated fetal calf serum, penicillin (100 U/ml), streptomycin (0·1 mg/ml) and glutamine (0·3 mg/ml)], all obtained from Invitrogen (Karlsruhe, Germany) was used as a standard medium (RPMI-SM). Jurkat T cells (E6-1, ATCC TIB152 and parental generated by Fanger *et al.*[40]), adherent growing HEK-293 cells and the murine hybridoma M195 secreting an anti-human CD33 immunoglobulin G (IgG) were purchased from the American Type Culture Collection (ATCC; Manassas, VA). HEK-293 cells adapted to suspension growth were kindly provided by Professor Wurm (EPFL Lausanne, Switzerland). The Chinese hamster ovary (CHO) cell line was kindly provided by Professor Chasin (Columbia University, New York, NY). The CHO cells expressing full-length CD33 antigen were generated as described previously[41] using the pEAK8 vector (Edge BioSystems, Gaithersburg, MD). Stably transfected cells were cultured in RPMI-SM + 2 μg/ml puromycin (Sigma, Munich, Germany). The complementary DNA (cDNA) coding for the scFv antibody recognizing the human CD3ε chain was kindly provided by Dr Thirion (Dr L Willems-Instituut, Diepenbeek, Belgium).[42] The cDNA coding for the scFv antibody recognizing human CD19 antigen was kindly provided by Professor Zola (Child Health Research Institute, Women's and Children's Hospital, Adelaide, South Australia).[43]

Isolation and cell culture of primary human T cells

Peripheral blood mononuclear cells (PBMC) used for the proliferation and cytotoxic assays were collected from

healthy donors and purified as previously described.[44] PBMC used for Ca^{2+} imaging experiments were purified from leucocyte reduction filters obtained from the local blood bank. Cells were collected by back-flushing the filter with 60 ml Hanks' balanced salt solution (HBSS; PAA, #15-009) and the peripheral blood lymphocytes (PBL) were isolated by a density gradient centrifugation at 450 ***g*** for 30 min at room temperature (Ficoll-Paque™plus; Amersham Biosciences, Freiburg, Germany; #17144002) in 50-ml Leucosep tubes (Greiner, Frickenhausen, Germany; #227290). The PBL layer was washed in HBSS. The remaining red blood cells were removed by the addition of 1 ml lysis buffer (155 mM NH_4Cl, 10 mM $KHCO_3$, 0·1 mM ethylenediaminetetraacetic acid, pH 7·3) for 1 min. After lysis, the cells were washed with HBSS (200 ***g***, 10 min, room temperature). For further purification, the PBL were resuspended in phosphate-buffered saline (PBS)/0·5% bovine serum albumin (BSA) and $CD4^+$ T cells were negatively isolated using the $CD4^+$ Negative Isolation kit (to avoid pre-stimulation) from Invitrogen (#113.17D) following the manufacturer's instruction. After isolation, the purity of the $CD4^+$ populations was analysed by fluorescence microscopy [anti-CD4/R-phycoerythrin (RPE) -conjugated antibody; Dako, Hamburg, Germany; #R0805]. $CD4^+$ cells were cultured in AIMV medium (Invitrogen, #12055-091) supplemented with 10% fetal calf serum. To generate effector cells from the primary naïve $CD4^+$ cells, the cells were either incubated with anti-CD3/anti-CD28-coated beads or with 12 U/ml human interleukin-2 (hIL-2; Roche, Mannheim, Germany) and 3 μg/ml phytohaemagglutinin (PHA, Sigma).[23]

Cloning of fusion proteins

The cDNA sequences coding for the extracellular domains of CD80 and CD86 were amplified from human PBMC using standard reverse transcription–polymerase chain reaction (RT-PCR) technology as described elsewhere.[44] The variable heavy chain (HC) and light chain (LC) sequences of anti-human CD33 antibodies[45] were amplified by PCR using specific primers including restriction sites (*Nco*I–*Hin*dIII for HC, *Eco*RV–*Bam*HI for LC) compatible with the pHOG expression vector and expressed as scFv fragments. Bi-specific fusion proteins and bi-specific double single-chain fragment variable (dscFv) constructs were obtained by introducing a 15-base-pair sequence coding for the five-amino-acid (G4S) linker between the two molecules of interest. Soluble CD33 antigen was obtained by RT-PCR amplifying the cDNA sequence coding for the extracellular domain of the CD33 antigen. The 3′ primer was extended by a HIS tag sequence suitable for immobilized metal affinity chromatography (IMAC). The entire sequence including the tag part was then transferred into the pEAK8 vector for protein production by transient gene expression.

Expression and purification of recombinant proteins

All recombinant proteins were expressed using the pEAK8 vector for transient gene expression in HEK-293 cells as described[46] using calcium phosphate transfection. Depending on the cell viability, culture supernatants were collected after 5–7 days and proteins were purified by HIS-tag chromatography.[47] Integrity and purity of recombinant proteins were checked by Coomassie gel and Western blot using the murine anti-myc tag 9E10 antibody (Roche) as previously described.[48]

Binding analysis

The binding properties of all fusion proteins carrying the scFv anti-CD33 were first assessed by enzyme-linked immunosorbent assay using an indirect detection system on CD33-antigen-coated plates. Ninety-six-well flat-bottom microtitre plates (MaxiSorp Immuno; Thermo Fisher Scientific, Langenselbold, Germany) were coated (overnight at 4°) with 2 μg/ml recombinant CD33 antigen in 50 μl coating buffer per well.[44] Plates were then blocked (with 2% milk powder in PBS for 2 hr at 37°), washed and incubated with varying dilutions of indicated fusion proteins (1 hr, room temperature). Bound molecules were detected by the 9E10 antibody (2 μg/ml, 1 hr, room temperature) and a horseradish peroxidase-conjugated/anti-mouse IgG as secondary antibody (dilution 1 : 1000; Dako). Detection was performed using *O*-phenylenediamine substrate (Sigma). Reaction was stopped with 3 M HCl, and plates were analysed using a fluorometer (model 1420, Victor 2; PerkinElmer, Wiesbaden, Germany) at 490 nm. Flow cytometry was performed as previously described.[41] In brief, 1×10^6 cells were incubated with the purified constructs of the indicated specificity and concentration (30 min, 4°). For the analysis of binding of fusion proteins, cells were then washed twice with PBS, incubated with 9E10 antibody (10 μg/ml, 1 hr, room temperature), and, finally, the complex was visualized by adding PE-conjugated goat anti-mouse serum (dilution 1/100, DakoCytomation). A mouse anti-human CD28 IgG antibody was used as a control (dilution 1/100; BD Bioscience, Heidelberg, Germany). Ten thousand cells of each sample were counted. Analysis was performed on a FACScan using CellQuest software as recommended by the manufacturer (BD Bioscience).

T-cell proliferation

The 96-well flat-bottom microtitre plates (MaxiSorp Immuno; Nunc) were coated (overnight at 4°) with 2 μg/ml of soluble recombinant CD33 antigen in 100 μl of coating buffer per well.[44] Plates were then blocked (with 120 μl of 2% milk powder in PBS for 2 hr at 37°), washed and incubated with varying dilutions of the indicated

fusion proteins (1 hr, room temperature). Unbound antibody molecules were then washed off and the plates were covered with 100 μl medium containing 100 000 PBMC. Proliferation was quantified as described previously.[49] Briefly, cells were pulsed with 1 μCi [^{3}H]thymidine (Amersham Pharmacia Biotech, Munich, Germany) per well for 16 hr after a 72-hr culture period. Cells were then harvested onto filter membranes using an Inotech cell harvester (Inotech AG, Dietikon, Switzerland), and proliferation was measured as counts per minute (c.p.m.) of incorporated [^{3}H]thymidine using a Wallac β-Counter 1450 Microbeta TriLux (PerkinElmer, Wiesbaden, Germany). All experiments were carried out in triplicate.

Cellular cytotoxicity assays

T-cell-dependent cytotoxicity was measured by an indirect cellular assay. All procedures were performed under sterile conditions using filtered reagents. Viable CD33 antigen-transfected CHO cells were plated on 96-well flat-bottom plates at a density of 5000 cells per well. Twenty-four hours later, the plates were washed thoroughly to remove all non-adherent cells and then co-incubated with varying dilutions of the indicated fusion proteins (1 hr, room temperature). Negative controls (dscFv anti-CD3/anti-CD19) and positive controls (1% Triton X-100) were also included in every experiment. Plates were washed again with PBS and wells were covered with 100 μl medium containing 100 000 PBMC, resulting in an estimated PBMC to CD33-transfected CHO cell ratio of 10 : 1 (assuming a doubling time of 24 hr for CHO cells). Plates were then cultured for 4 days in an incubator under standard conditions. The T cells and the dead CHO cells were washed off, and the number of the remaining living CHO cells was determined by their ability to reduce a tetrazolium salt to coloured formazan following the instructions provided by the manufacturer (EZ4U Proliferation Assay; Biomedica, Germany). The percentage of cytotoxicity was calculated from the following equation:

$$(A_{\text{Experimental value}} - A_{\text{negative control}})/(A_{\text{positive control}} - A_{\text{negative control}}) \times 100$$

where $A_{\text{Experimental value}}$ is the absorbance with the sample, $A_{\text{negative control}}$ is the absorbance with dscFv anti-CD3/anti-CD19, and $A_{\text{positive control}}$ is the absorbance with 1% Triton X-100. All assays were performed in triplicate.

Immunofluorescence

Between $0{\cdot}5 \times 10^6$ and 1×10^6 T cells were coated on glass cover slips (diameter 12 mm) with polyornithine (0·1 mg/ml), washed twice, fixed by incubating them for 20 min in PBS/3% paraformaldehyde, and incubated for 3 min in PBS/0·1 M glycine. For CTLA-4 staining, cells were permeabilized by incubating them for 20 min in PBS/0·1% Triton. Before antibody staining, cells were blocked by incubating them for 20 min in blocking buffer [PBS/2% BSA/with (CTLA-4) or without (CD28) 0·1% Triton]. Cells were then stained for 60 min with a 1 : 10 dilution of R-PE-labelled anti-CTLA-4 (BD Bioscience) or anti-CD28 (Ebioscience, Hatfield, UK) antibodies. After washing the cells three times, they were embedded using a ProLong® Antifade kit (Invitrogen).

Immunofluorescence measurements were carried out with an epifluorescence system or with a confocal system as described elsewhere.[23,50,51] The epifluorescence system was an Olympus IX 70 microscope (Olympus) equipped with either a 20 × (UApo/340, N.A. 0.75) or a 40 × (Uplan/Apo, N.A. 1.0) objective. For confocal imaging, a Nipkow-disc-based scanning head (QLC-100; Visitech, Sunderland, UK) was attached to an upright microscope (Eclipse 600; Nikon, Düsseldorf, Germany) equipped with a 100 × water lens (Plan 1.1; Nikon). The light source was a 488 nm solid-state laser (Sapphire 488-30; Coherent, Dieburg, Germany).

Single cell Ca^{2+} imaging

Between 2×10^5 and 5×10^5 CHO cells were seeded on glass cover slips 2–3 days before the experiments. Immediately before Ca^{2+} imaging, the cells were incubated with the particular concentration of fusion proteins in 50 μl culture medium and washed afterwards with culture medium with 10 mM HEPES added. Glass cover slips were mounted on the stage of an Olympus IX 70 microscope equipped with a 20 × (UApo/340, N.A. 0·75) objective in a self-made recording chamber, which allowed a complete solution exchange < 1 second. In parallel, T cells were loaded at 22–23° for 30 min with 2 μM fura-2/acetoxymethyl ester (AM) (Invitrogen) in culture medium with 10 mM HEPES added, washed with fresh medium, and immediately used. T cells were then added and cells were alternately illuminated at 340 and 380 nm with the Polychrome IV monochromator (TILL Photonics, Gräfelfing, Germany) and with an infrared light source using SP 410 as excitation filter and DCLP 410 as dichroic mirror. The fluorescence emissions at $\lambda > 440$ nm (LP 440) were captured with a CCD camera (TILL Imago), digitized, and analysed using TILL VISION software. Ratio images were recorded at intervals of 5 seconds. In some experiments thapsigargin (TG, 1 μM) was used to completely empty the stores.

Statistical analysis

EXCEL, IGOR PRO and TILL VISION were used for data analysis. An unpaired, two-sided Students *t*-test was used to test for significance.

Results

Bi-specific recombinant fusion proteins

All fusion proteins were generated as single chain molecules to prevent any false pairing or degradation (Fig. S1). The extracellular domains of CD80 and CD86 were cloned at the N-terminal end of the scFv anti-CD33 to ensure correct binding to their respective receptors.[52] Soluble proteins were produced in HEK-293 cells by transient gene expression with a yield of 0·5–2 mg total protein/l of cell culture supernatant, purified by IMAC and checked by Coomassie and Western blot analysis for purity and integrity. Proper binding for all fusion proteins was tested by enzyme-linked immunosorbent assay on recombinant CD33 antigen (data not shown) and flow cytometry (Fig. S2) on either CD33-transfected CHO or Jurkat T cells. Binding of the scFv anti-CD33 was not altered in any of the fusion proteins when compared with the parental scFv anti-CD33. The scFv anti-CD3 and the extracellular domains of CD80 and CD86 showed a moderate to weak binding affinity to their respective receptors. The dscFv anti-CD3/anti-CD19 were used as control.

Costimulation by CD86 but not by CD80 cross-linking is very efficient at increasing T-cell proliferation and T-cell killing capacity

The dscFv anti-CD33/anti-CD3 construct induced proliferation of naïve T cells in the presence of the CD33 antigen in a dose-dependent manner (Fig. 1). Proliferation was only seen when cross-linking of CD3 molecules was achieved by dscFv antibodies that were immobilized by the CD33 antigen. The soluble anti-CD3 antibodies had no effect on T-cell proliferation (data not shown). In addition, neither the scFv anti-CD33 by itself nor any of the fusion proteins carrying the costimulatory molecules was able to induce proliferation (Fig. 1). Suboptimal T-cell proliferation was observed at concentrations smaller than 5 μg/ml dscFv anti-CD33/anti-CD3. The combination of 10 μg/ml sc CD80/anti-CD33 fusion protein with the suboptimal concentration of 2 μg/ml dscFv anti-CD33/anti-CD3 did not significantly enhance T-cell proliferation above that seen with dscFv anti-CD33/anti-CD3 alone (Fig. 2a). In contrast, T-cell proliferation was significantly increased by the combination of 2 μg/ml dscFv anti-CD33/anti-CD3 and 10 μg/ml sc CD86/anti-CD33

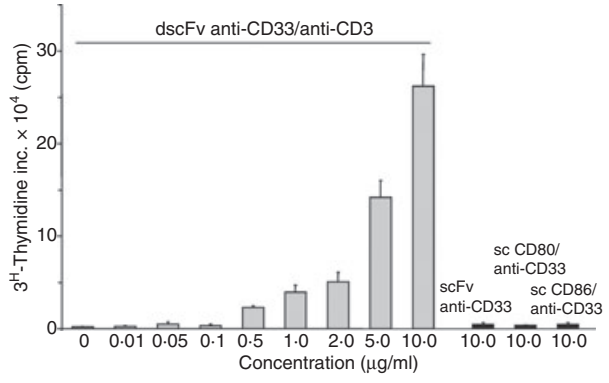

Figure 1. Double single-chain fragment variable antibodies (dscFv) anti-CD33/anti-CD3 induced proliferation of T cells in a dose-dependent manner. Antigen-immobilized dscFv anti-CD33/anti-CD3 at various concentrations or control antibody fusion proteins single-chain fragment variable (scFv) anti-CD33, sc CD80/anti-CD33 and sc CD86/anti-CD33 (10 μg/ml) were used to stimulate T cells for 3 days. Cells were then pulsed for 16 hr before harvesting. Mean values of triplicate cultures are shown. Results are representative of three independent experiments. c.p.m., counts per minute.

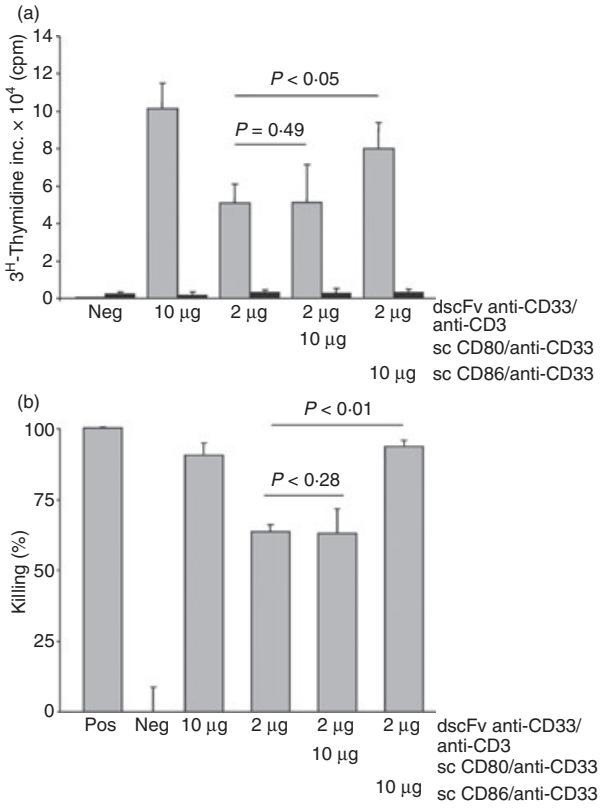

Figure 2. CD86 but not CD80 increased T-cell proliferation and cytotoxicity. (a) Suboptimal doses of double single-chain fragment variable (dscFv) anti-CD33/anti-CD3 (2 μg/ml) and 10 μg/ml of costimulatory molecules, either sc CD80/anti-CD33 or sc CD86/anti-CD33, were used to initiate the proliferation of the cytotoxic activity of naïve T cells in the presence of immobilized CD33 antigen (grey column) or phosphate-buffered saline (PBS; black column). The dscFv anti-CD19/anti-CD3 served as negative control (Neg). c.p.m., counts per minute. (b) Same constructs as in (a) were used. *P*-values for the difference between absence and presence of costimulatory molecules are indicated. Negative controls (Neg, dscFv anti-CD19/anti-CD3) and positive controls (Pos, 1% Triton X-100) were included in every experiment. Results are representative of three independent experiments.

($P < 0{\cdot}05$) and reached levels that were comparable with the higher doses of dscFv anti-CD33/anti-CD3 (10 μg/ml).

Another functionally important T-cell activation parameter is their ability to kill target cells. In agreement with the proliferation data, concentrations of dscFv anti-CD33/anti-CD3 smaller than 5 μg/ml induced a suboptimal level of T-cell cytotoxicity when compared with 10 μg/ml dscFv anti-CD33/anti-CD3. However, the level of cytotoxicity could be significantly enhanced by adding 10 μg/ml sc CD86/anti-CD33 to 2 μg/ml dscFv anti-CD33/anti-CD3 (Fig. 2b). Under these conditions cytotoxicity levels were almost identical to the levels achieved with 10 μg/ml dscFv anti-CD33/anti-CD3. Only a small and insignificant increase in T-cell cytotoxic activity could be observed when 10 μg/ml sc CD80/anti-CD33 fusion protein was added to 2 μg/ml dscFv anti-CD33/anti-CD3. This difference between CD86 and CD80 costimulation was not only restricted to the single dose of 10 μg/ml but was also seen over an entire dose range (0·01–10 μg/ml; data not shown).

CD86 costimulation induces larger Ca^{2+} signals than CD80 costimulation

The magnitude of Ca^{2+} influx has been shown to correlate with T-cell proliferation[23,28] so we tested the hypothesis that differences in Ca^{2+} signalling are responsible for differences in T-cell activation observed during costimulation. To analyse Ca^{2+} signals in single cells following costimulation, we established conditions that allowed us to measure Ca^{2+} signals in primary T cells following stimulation by bi-specific antibody-loaded CHO cells (Fig. 3a). Contact between T cells and CHO cells that were preloaded with dscFv anti-CD33/anti-CD3 (used at 2 μg/ml from now on) induced Ca^{2+} signals in almost all cells, whereas cells with no contact showed no Ca^{2+} signals. The ratio 340/380, which is proportional to $[Ca^{2+}]_i$, is shown over time for one T cell that makes a CHO-cell contact and one T cell that makes no CHO-cell contact (Fig. 3b). We observed $[Ca^{2+}]_i$ rises only in cells with contact, but not in cells with no contact or in cases when only costimulatory antibodies were used (Fig. S3). To the best of our knowledge, this method is the most efficient focal stimulation method to induce Ca^{2+} signals in non-clonal human T-cell populations.

We next analysed whether costimulation with sc CD86/anti-CD33 or sc CD80/anti-CD33 antibodies (used at 10 μg/ml from now on) could increase Ca^{2+} signals following focal stimulation by pre-loaded CHO cells. Analysing parental Jurkat T cells (Fig. 4a), E6-1 Jurkat T cells (Fig. 4b) or naïve, unstimulated primary $CD3^+$ T cells (Fig. 4c), we could not observe any significant differences between stimulation with dscFv anti-CD33/anti-CD3 alone or in combination with sc CD80/anti-CD33 or sc CD86/anti-CD33. However, the differences with respect to the proliferation and the killing capacity between dscFv anti-CD33/anti-CD3 with or without costimulation (Figs 1, 2) were always analysed after 4 days. During this time, T cells had reached effector status. In a next step, we mimicked these conditions. To generate effector T cells without exposing them to dscFv anti-CD33/anti-CD3 before the actual Ca^{2+} imaging experiment, naïve T cells were stimulated either with PHA and IL-2 or with anti-CD3/anti-CD28-coated beads. We have previously shown that this protocol generates an almost pure effector T-cell population.[23] We repeated the Ca^{2+} imaging

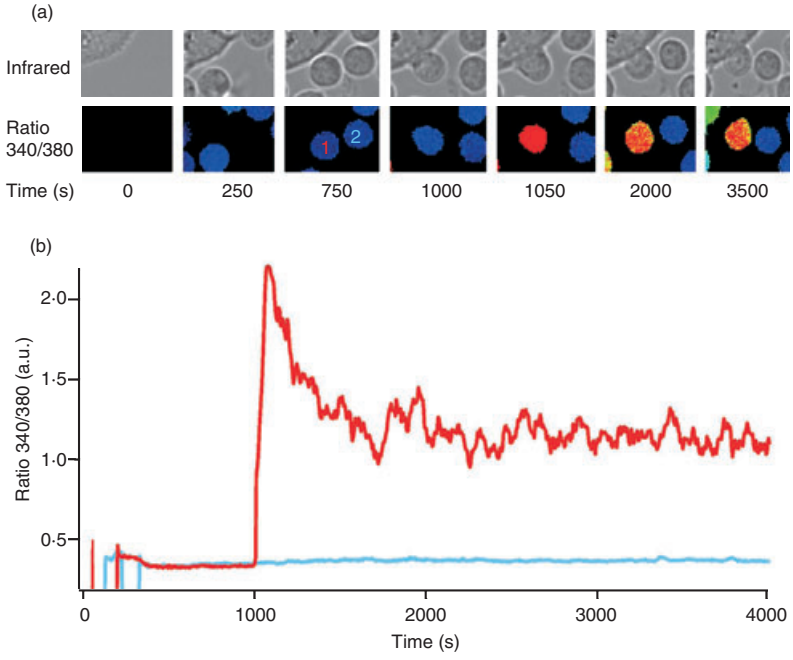

Figure 3. Chinese hamster ovary (CHO) cells loaded with double single-chain fragment variable (dscFv) anti-CD33/anti-CD3 increase Ca^{2+} concentration in $CD4^+$ T-cells. (a) Infrared and $[Ca^{2+}]_i$ (as ratio 340/380) images. T cells are visible by the fura-2/AM loading in the ratio 340/380 pictures and in the infrared channel whereas CHO cells are only visible in the infrared channel. T cell 1 makes contact with a CHO cell, red Ca^{2+} trace in (b), whereas T-cell 2 makes no contact with a CHO cell during the entire experiment, blue Ca^{2+} trace in (b). (b) $[Ca^{2+}]_i$ kinetics from typical fura-2/AM-loaded $CD4^+$ T-cells either stimulated (T-cell 1, red trace) or not stimulated (T-cell 2, blue trace) by CHO cells loaded with 2 μg/ml dscFv anti-CD33/anti-CD3 in 0·25 mM Ca^{2+} solution. $[Ca^{2+}]_i$ and infrared images were recorded in parallel every 5 seconds.

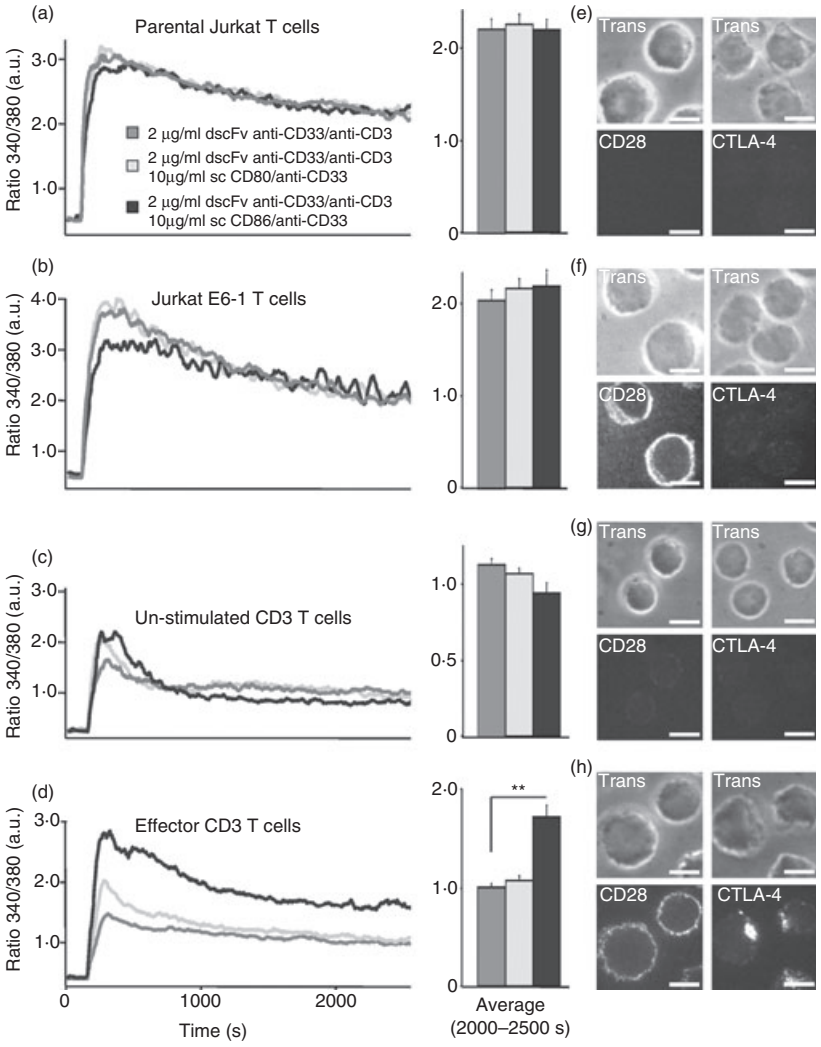

Figure 4. CD86 costimulation increases net Ca^{2+} entry in effector T cells. (a–d) Kinetics of intracellular [Ca^{2+}] (as ratio 340/380) of parental Jurkat T cells, E6-1 Jurkat T cells, naïve, unstimulated primary $CD4^+$ T cells or effector T cells. Effector T cells were prestimulated for 4 days with phytohaemagglutinin and interleukin-2. Cells were stimulated by Chinese hamster ovary (CHO) cells loaded with 2 μg/ml of dscFv anti-CD33/anti-CD3 alone or together with 10 μg/ml of sc CD80/anti-CD33 or sc CD86/anti-CD33. (e–h) CD28 and a cytotoxic T-lymphocyte antigen 4 (CTLA-4) staining of the corresponding cell type are shown. Scale bars represent 5 μm (**$P < 0{\cdot}01$).

experiments with these effector T cells and observed clear differences between stimulation with dscFv anti-CD33/anti-CD3 alone and stimulation with dscFv anti-CD33/anti-CD3 in combination with the costimulatory molecules. Stimulation of the effector T cells with dscFv anti-CD33/anti-CD3 in combination with sc CD86/anti-CD33 induced larger Ca^{2+} signals than dscFv anti-CD33/anti-CD3 in combination with sc CD80/anti-CD33 or dscFv anti-CD33/anti-CD3 alone (Fig. 4d), which matches with the proliferation and cytotoxicity data shown in Figs 1 and 2.

Because CD28 and CTLA-4 are the main receptors for CD80 and CD86 on T cells, we analysed their expression. We did not detect significant CD28 expression on parental Jurkat T cells, however, it was clearly expressed on E6-1 Jurkat T-cells (Fig. 4e,f). It was also modestly expressed on naïve T cells but up-regulated during T-cell maturation, following stimulation of naïve T cells with IL-2 and PHA or anti-CD3/anti-CD28-coated beads (Fig. 4g,h). There was no detectable CTLA-4 surface expression on both Jurkat T-cell lines (Fig. 4e,f) and naïve T cells (Fig. 4g) but there was a clear up-regulation during T-cell maturation (Fig. 4h).

CD28 is recruited to the immunological synapse (IS) even in the absence of CD80 or CD86 costimulation. However, its localization at the IS can be disrupted by CTLA-4, which needs ligand binding to be recruited to the IS.[37] Costimulation should therefore influence effector T-cell signalling much more than signalling in naïve cells because only effector cells express CD28 and CTLA-4 at high levels. This is indeed the case as shown in Fig. 4(d,h).

Interfering with the function of CD28 should cancel the difference between CD80 and CD86 costimulation in effector T cells. We applied an antibody blocking CD28 function, which abrogated the differences between sc CD80/anti-CD33 and sc CD86/anti-CD33 costimulation in Ca^{2+} measurements (Fig. 5). In summary, we conclude that both, CD28 and CTLA-4 (at least through its regulation of CD28 at the IS), are required for the different efficiencies of CD80 and CD86 costimulation.

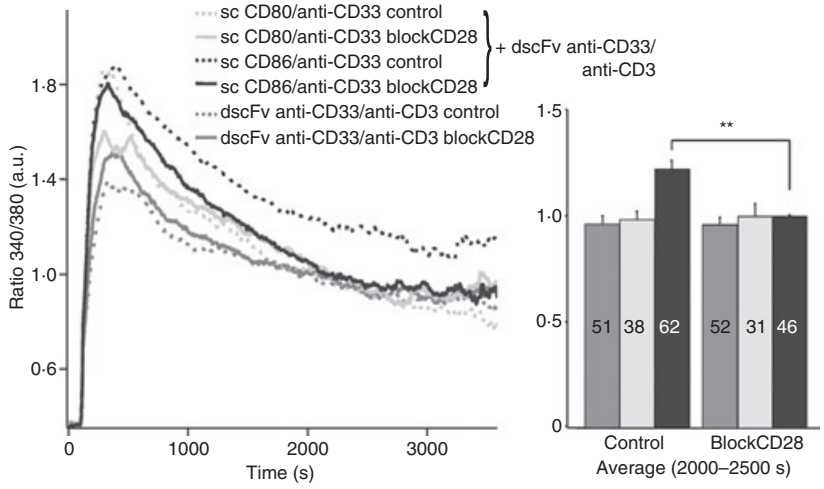

Figure 5. An inhibitory anti-CD28 antibody abrogated the differences between single-chain (sc) CD80/anti-CD33 or sc CD86/anti-CD33 costimulation. Kinetics and quantification of intracellular [Ca^{2+}] (as ratio 340/380) of $CD4^+$ T cells stimulated by CHO cells loaded with 2 μg/ml double single-chain fragment variable (dscFv) anti-CD33/anti-CD3 alone or together with 10 μg/ml sc CD80/anti-CD33 or sc CD86/anti-CD33. $CD4^+$ T-cells were prestimulated with anti-CD3/anti-CD28-coated beads for 4 days. Cells were incubated for 10 min with the inhibitory anti-CD28 antibody in a 1 : 20 solution before measurement. The numbers of cells are given in the bars (**$P < 0{\cdot}01$).

CD86 costimulation increases net Ca^{2+} entry

The increased Ca^{2+} signals observed after sc CD86/anti-CD33 costimulation compared with sc CD80/anti-CD33 costimulation can, in principle, be a result of two general mechanisms: increased Ca^{2+} release or increased net Ca^{2+} influx. To test this, we separated Ca^{2+} release and Ca^{2+} influx. The Ca^{2+} release was not different when induced by dscFv anti-CD33/anti-CD3 in combination with sc CD86/anti-CD33 compared with dscFv anti-CD33/anti-CD3 in combination with sc CD80/anti-CD33 (Fig. 6a). The figure also shows that Ca^{2+} release between different donors was extremely homogeneous (Fig. 6b), which was also the case for the influx (data not shown). Both, costimulation with CD80 and CD86 emptied the Ca^{2+} stores equally well. To analyse Ca^{2+} influx independently of Ca^{2+} release, we compared Ca^{2+} influx after the full depletion of Ca^{2+} stores. The TG was used to fully deplete Ca^{2+} stores after the initial stimulation with the different bi-specific antibodies. Because Ca^{2+} release by costimulation does not occur simultaneously in the cells (in Fig. 6 all cells were aligned to the initiation of the Ca^{2+} release), only a slight but inhomogeneous Ca^{2+} signal during the release phase could be observed. In cells with a clear Ca^{2+} release after costimulation, no further Ca^{2+} release by TG was detected indicating that TG-sensitive stores were already fully depleted by the costimulation (Fig. 7). While the Ca^{2+} release was not influenced by costimulation, the Ca^{2+} influx was clearly different, as was evident after Ca^{2+} re-addition. The dscFv anti-CD33/anti-CD3 in combination with sc CD86/anti-CD33 induced a larger Ca^{2+} entry in comparison with dscFv anti-CD33/anti-CD3 in combination with sc CD80/anti-CD33. This indicates that costimulation increases Ca^{2+} influx independent of Ca^{2+} release. Export rates of Ca^{2+} were not different for both costimulation methods (data not shown). We conclude that the different amplitudes of Ca^{2+} signals following dscFv anti-CD33/anti-CD3 in combination with sc CD86/anti-CD33 when compared with dscFv anti-CD33/anti-CD3 in combination with sc CD80/anti-CD33 can only be explained by differences in net Ca^{2+} entry but are independent of Ca^{2+} release.

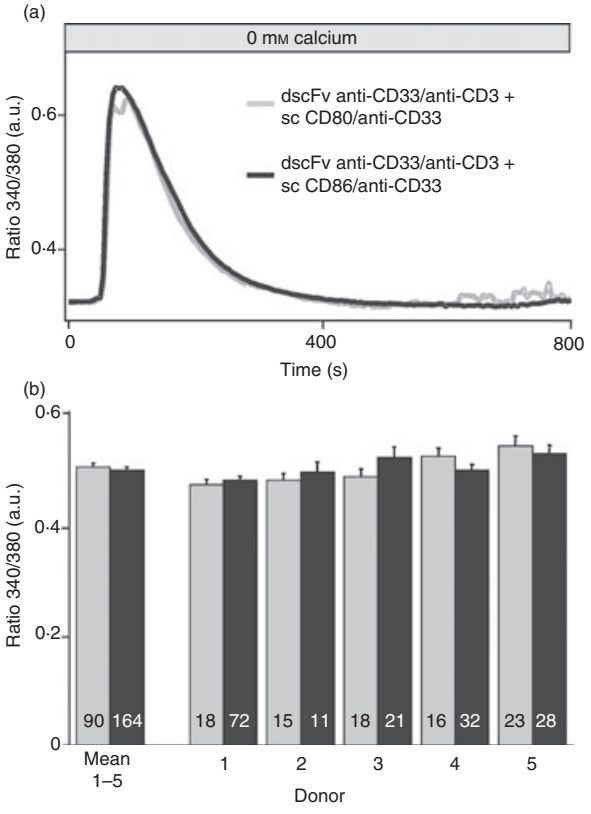

Figure 6. Ca^{2+} release was identical for CD80 and CD86 costimulation. (a) Intracellular [Ca^{2+}] (as ratio 340/380) of $CD4^+$ T cells stimulated by Chinese hamster ovary (CHO) cells loaded with 2 μg/ml double single-chain fragment variable (dscFv) anti-CD33/anti-CD3 together with 10 μg/ml sc CD80/anti-CD33 or sc CD86/anti-CD33 following store depletion in the absence of extracellular Ca^{2+}. The time-point zero was defined for every cell as 100 seconds before the release started. (b) Bars show the average of five different donors and all five donors individually (cell numbers are given in the bars).

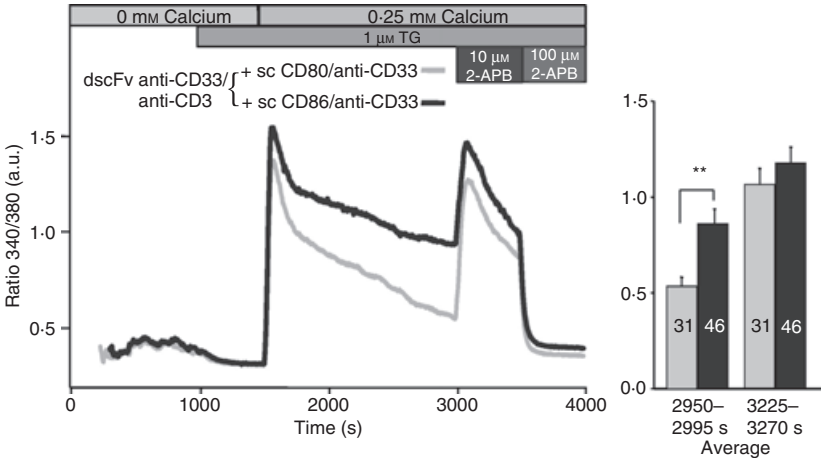

Figure 7. The differences in Ca^{2+} influx were eliminated by the application of 10 μM 2-aminoethyldiphenyl borate (2-APB). Kinetics of intracellular $[Ca^{2+}]$ (as ratio 340/380) of $CD4^+$ T cells stimulated by Chinese hamster ovary (CHO) cells loaded with 2 μg/ml double single-chain fragment variable (dscFv) anti-CD33/anti-CD3 together with 10 μg/ml sc CD80/anti-CD33 or sc CD86/anti-CD33. $CD4^+$ T cells were pre-stimulated with anti-CD3/anti-CD28-coated beads for 5 days. After 1000 seconds, cells were treated with thapsigargin (TG) in the absence of extracellular Ca^{2+} to completely deplete Ca^{2+} stores. A Ca^{2+} concentration of 0.25 mM was added to analyse Ca^{2+} entry. Finally, 10 μM 2-APB and 100 μM 2-APB were added. Numbers of analysed cells are given in the bars. (**$P < 0{\cdot}01$).

Soboloff *et al.*[19] and Parvez *et al.*[21] discovered that STIM2 can inhibit CRAC channel activity. In addition, Parvez *et al.* showed that STIM2 can also activate a store-independent mode of CRAC/ORAI channels. The store-independent mode of CRAC activation was also observed following the application of low concentrations of 2-aminoethyldiphenyl borate (2-APB) in STIM2/ORAI1 over-expressing HEK-293 cells and in ORAI3 over-expressing HEK-293 cells.[53] Concentrations of 2-APB up to 10 μM have previously been shown to transiently facilitate CRAC currents in T cells.[54] To test if STIM2 and/or ORAI3 activity could be responsible for the differences in costimulation, we compared the effect of 10 μM 2-APB on Ca^{2+} signals in $CD4^+$ T-cells (Fig. 8). The application of 10 μM 2-APB increased Ca^{2+} signals to similar values for both conditions indicating that a difference in the store-independent mode of CRAC channel activation might be the reason for the observed differences between stimulation with dscFv anti-CD33/anti-CD3 in combination with sc CD86/anti-CD33 when compared with dscFv anti-CD33/anti-CD3 in combination with sc CD80/anti-CD33. 100 μM 2-APB decreased Ca^{2+} influx as previously reported.[54] The costimulation effect on Ca^{2+} influx and the effect of 2-APB were independent of TG because we obtained similar results in the absence of TG (Fig. 8). We conclude that store-independent Ca^{2+} entry mediated by STIM2 and/or ORAI3 is likely to be involved in the costimulation-dependent regulation of CRAC channel activity.

Discussion

We show evidence that T-cell costimulation by CD80 or CD86 ligand binding causes differences in net Ca^{2+} entry

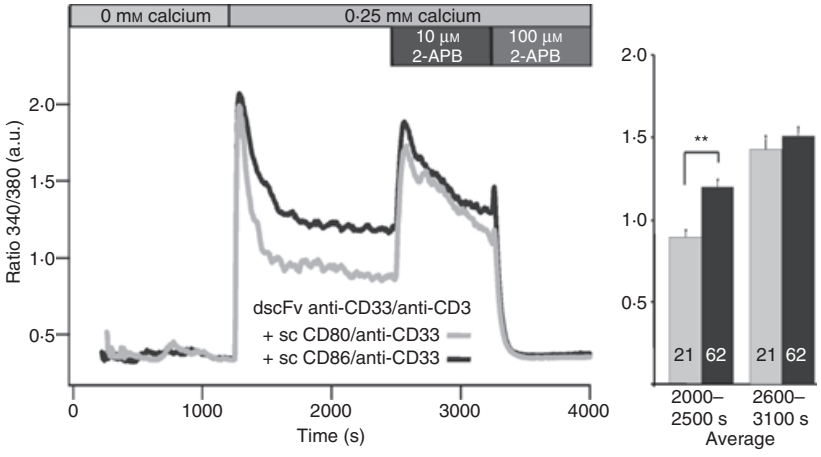

Figure 8. The differences in Ca^{2+} influx were eliminated by the application of 10 μM 2-aminoethyldiphenyl borate. Same as Fig. 7, only that thapsigargin was omitted. Numbers of analysed cells are given in the bars (**$P < 0{\cdot}01$).

depending on the activation state of the T-cell. The differences of Ca^{2+} entry are not linked to Ca^{2+} store depletion, offering a potential physiological function for store-independent Ca^{2+} entry. Store-independent Ca^{2+} entry by CRAC channels has recently been proposed;[21,53] however, so far, no physiological function has been assigned. Our data reveal that the store-independent mode of CRAC may be important to distinguish different modes of costimulation.

The interaction of CD80 or CD86 with CD28 or CTLA-4 has been established in the early 1990s as the first pathway of T-cell costimulation and co-inhibition and has since been the subject of intense studies.[55] The initial work using CD80 or CD86 transfected cell lines was replaced in many studies by CD28-specific monoclonal antibodies because they showed adequate T-cell proliferation in the presence of suboptimal stimulation by TCR cross-linkage. However, anti-CD28 antibodies provide a rather simplistic model for costimulation because they have a different binding pattern on the CD28 molecule and affinity when compared with the natural CD80 or CD86 ligand,[33,34,56,57] More importantly, CD28-specific antibodies do not provide any information on the subtle differences between CD80- and CD86-mediated costimulation and cannot mimic the spatial and temporal differences involved in CD28 and CTLA-4 signalling. CD28 is recruited to the IS even in the absence of CD80 or CD86 costimulation and its localization at the IS can be disrupted by CTLA-4, which needs ligand binding to be recruited to the IS.[37] Costimulation should, therefore, influence effector T-cell signalling more severely than signalling in naïve T cells because only effector cells express both CD28 and CTLA-4 at high levels.

We have linked these findings with our Ca^{2+} data and developed the following hypothesis (Fig. 9). The Ca^{2+} signals are caused by TCR-dependent stimulation of store-dependent CRAC/ORAI1 channels (Fig. 9a,b) in a STIM1-dependent manner and by CD28-dependent store-independent activation of Ca^{2+} entry, potentially in a STIM2/ORAI1 or ORAI3-dependent manner. The CD28-dependent Ca^{2+} entry can occur in the context of the IS formation. If only CD28 is expressed, we would therefore not expect differences in Ca^{2+} signals between CD80 or CD86 costimulation because CD28 is recruited to the IS independent of the type of costimulation (Fig. 9a). This is the case in Jurkat E6-1 and naïve primary T cells. However, if both CD28 and CTLA-4 are present at high concentrations, as in the case of effector T cells, it is expected that CD80 should preferentially bind to CTLA-4 and not so much to CD28, with the opposite being true for CD86.[37] Therefore, CD86 should enhance CD28 recruitment to the IS and CD80 should inhibit CD28 recruitment by recruiting CTLA-4 instead. Through an unknown mechanism CD86, but not CD80, somehow enhances the store-independent activation of the CRAC channel,[21,53] most likely in

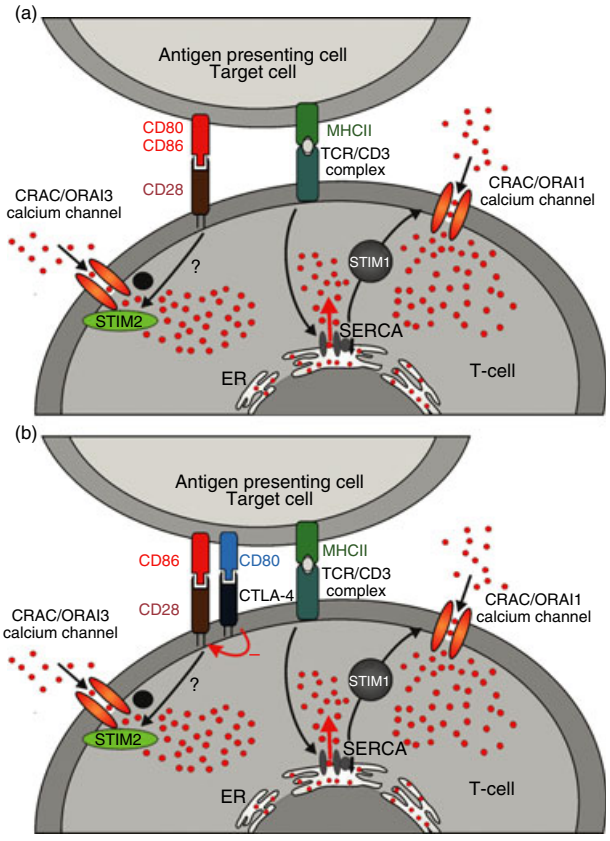

Figure 9. A model for the activation of store-independent Ca^{2+} entry by costimulation is shown. Details are discussed in the text.

a STIM2/ORAI1 and/or ORAI3-dependent manner (Fig. 9b). In this model, the negative effect of CTLA-4 on T-cell activation is caused by the inhibition of CD28 recruitment to the IS.

The knowledge of the fine-tuned difference in T-cell activation mediated by costimulatory molecules is of utmost importance not only to understand the underlying biology, but may also lead to novel therapeutic strategies that aim to activate the immune system against infectious and malignant diseases. Super-agonistic antibodies targeting costimulatory molecules and activating T cells by bypassing the first signal have been developed in recent years.[58] These super-agonistic antibodies bind to receptor domains that are not physiologically recognized by naturally occurring ligands, circumvent the need for TCR specificity and, most importantly, are no longer regulated by the human immune system. This last issue has recently gained significant attention because a clinical trial using a CD28 super-agonistic antibody (TGN1412) confirmed in a dramatic manner that no model systems exists today that can predict immune mechanisms induced by super-agonistic molecules.[58] In an early clinical trial performed in healthy volunteers, it was expected that activation of regulatory T cells by TGN1412 would further suppress the immune system and that the antibody would, eventually, be developed to

treat patients with autoimmune diseases. As the CD28 antigen is expressed on the vast majority of T cells and not only on the small proportion of regulatory T cells, a broad T-cell activation pattern was observed resulting in a life-threatening cytokine release syndrome requiring treatement in the intensive-care unit. This clinical experience has demonstrated that the nature of super-agonistic, non-physiological ligands is unpredictable when tested *in vivo*. Along that line, a CTLA4–immunoglobulin has been developed for blockage of the CD28-CD80/CD86 pathway. This fusion protein consists of the extracellular binding domain of CTLA-4 linked to a modified Fc domain of human IgG1 and serves as a competitive inhibitor of the CD28 pathway.[59] To optimize blockade of CD86 signalling as the more potent costimulatory pathway, site-directed mutagenesis was performed introducing two amino acid substitutions (L104E and A29Y) resulting in a fourfold slower off-rate for CD86 and a twofold slower off rate for CD80 when compared with the parental molecule. In addition, the final fusion protein demonstrated a 10-fold more potent inhibition of T-cell proliferation in a mixed lymphocyte reaction.[59] These data confirm that optimizing the binding pattern of ligands involved in the CD28/CTLA-4 costimulation/co-inhibition pathway is probably superior to the development of artificial binders. Considering the severe problems with stimulatory antibodies observed in clinical trials, our work is one important step forward to understand subtle differences in the signalling process between costimulatory molecules. Pinpointing the store-independent mode of CRAC/ORAI channel activation as a potential mediator for the differential activation by costimulation reveals a new target for more specific immune-suppressive inhibitors.

Acknowledgements

Research carried out for this study with human material has been approved by the local ethics committee. The authors have no conflict of interest. We thank Bettina Strauß and Anja Ludes for excellent technical support. We thank Varsha Pattu for reading and correcting the manuscript. This project was supported in part by the Ludwig Institute for Cancer Research, NY, USA (to A.M.S. and C.R.), Oncosuisse (to C.R.), the Deutsche Forschungsgemeinschaft (SFB 530, project A3, DFG grant HO 2190/1-2, and Graduate Colleges 'Molecular, physiological and pharmacological analysis of cellular membrane transport' and 'Calcium signaling and nanodomains', all to M.H.) and a competitive intra-faculty grant from HOMFOR (to E.C.S.).

References

1 Friedl P, den Boer AT, Gunzer M. Tuning immune responses: diversity and adaptation of the immunological synapse. *Nat Rev Immunol* 2005; **5**:532.

2 Jacobelli J, Andres PG, Boisvert J, Krummel MF. New views of the immunological synapse: variations in assembly and function. *Curr Opin Immunol* 2004; **16**:345.

3 Samelson LE. Signal transduction mediated by the T cell antigen receptor: the role of adapter proteins. *Annu Rev Immunol* 2002; **20**: 371.

4 Lanzavecchia A, Sallusto F. Antigen decoding by T lymphocytes: from synapses to fate determination. *Nat Immunol* 2001; **2**:487.

5 Crabtree GR, Olson EN. NFAT signaling: choreographing the social lives of cells. *Cell* 2002; **109**(Suppl):S67.

6 Parekh AB, Putney JW Jr. Store-operated calcium channels. *Physiol Rev* 2005; **85**:757.

7 Feske S. Calcium signalling in lymphocyte activation and disease. *Nat Rev Immunol* 2007; **7**:690.

8 Lewis RS. The molecular choreography of a store-operated calcium channel. *Nature* 2007; **446**:284.

9 Quintana A, Griesemer D, Schwarz EC, Hoth M. Calcium-dependent activation of T-lymphocytes. *Pflugers Arch* 2005; **450**:1.

10 Hoth M, Penner R. Depletion of intracellular calcium stores activates a calcium current in mast cells. *Nature* 1992; **355**:353.

11 Zweifach A, Lewis RS. Mitogen-regulated Ca^{2+} current of T lymphocytes is activated by depletion of intracellular Ca^{2+} stores. *Proc Natl Acad Sci U S A* 1993; **90**:6295.

12 Feske S, Gwack Y, Prakriya M *et al.* A mutation in Orai1 causes immune deficiency by abrogating CRAC channel function. *Nature* 2006; **441**:179.

13 Peinelt C, Vig M, Koomoa DL *et al.* Amplification of CRAC current by STIM1 and CRACM1 (Orai1). *Nat Cell Biol* 2006; **8**:771.

14 Prakriya M, Feske S, Gwack Y, Srikanth S, Rao A, Hogan PG. Orai1 is an essential pore subunit of the CRAC channel. *Nature* 2006; **443**:230.

15 Yeromin AV, Zhang SL, Jiang W, Yu Y, Safrina O, Cahalan MD. Molecular identification of the CRAC channel by altered ion selectivity in a mutant of Orai. *Nature* 2006; **443**:226.

16 Zhang SL, Yu Y, Roos J, Kozak JA, Deerinck TJ, Ellisman MH, Stauderman KA, Cahalan MD. STIM1 is a Ca^{2+} sensor that activates CRAC channels and migrates from the Ca^{2+} store to the plasma membrane. *Nature* 2005; **437**:902.

17 Roos J, DiGregorio PJ, Yeromin AV *et al.* STIM1, an essential and conserved component of store-operated Ca^{2+} channel function. *J Cell Biol* 2005; **169**:435.

18 Liou J, Kim ML, Heo WD, Jones JT, Myers JW, Ferrell JE Jr, Meyer T. STIM is a Ca^{2+} sensor essential for Ca^{2+}-store-depletion-triggered Ca^{2+} influx. *Curr Biol* 2005; **15**:1235.

19 Soboloff J, Spassova MA, Hewavitharana T, He LP, Xu W, Johnstone LS, Dziadek MA, Gill DL. STIM2 is an inhibitor of STIM1-mediated store-operated Ca^{2+} entry. *Curr Biol* 2006; **16**:1465.

20 Soboloff J, Spassova MA, Tang XD, Hewavitharana T, Xu W, Gill DL. Orai1 and STIM reconstitute store-operated calcium channel function. *J Biol Chem* 2006; **281**:20661.

21 Parvez S, Beck A, Peinelt C *et al.* STIM2 protein mediates distinct store-dependent and store-independent modes of CRAC channel activation. *FASEB J* 2007; **22**:752.

22 Oh-Hora M, Yamashita M, Hogan PG *et al.* Dual functions for the endoplasmic reticulum calcium sensors STIM1 and STIM2 in T cell activation and tolerance. *Nat Immunol* 2008; **9**:432.

23 Schwarz EC, Kummerow C, Wenning AS *et al.* Calcium dependence of T cell proliferation following focal stimulation. *Eur J Immunol* 2007; **37**:2723.

24 Gwack Y, Feske S, Srikanth S, Hogan PG, Rao A. Signalling to transcription: store-operated Ca^{2+} entry and NFAT activation in lymphocytes. *Cell Calcium* 2007; **42**:145.

25 Hogan PG, Chen L, Nardone J, Rao A. Transcriptional regulation by calcium, calcineurin, and NFAT. *Genes Dev* 2003; **17**:2205.

26 Feske S, Giltnane J, Dolmetsch R, Staudt LM, Rao A. Gene regulation mediated by calcium signals in T lymphocytes. *Nat Immunol* 2001; **2**:316.

27 Feske S, Prakriya M, Rao A, Lewis RS. A severe defect in CRAC Ca^{2+} channel activation and altered K^+ channel gating in T cells from immunodeficient patients. *J Exp Med* 2005; **202**:651.

28 Zitt C, Strauss B, Schwarz EC, Spaeth N, Rast G, Hatzelmann A, Hoth M. Potent inhibition of Ca^{2+} release-activated Ca^{2+} channels and T-lymphocyte activation by the pyrazole derivative BTP2. *J Biol Chem* 2004; **279**:12427.

29 Partiseti M, Le Deist F, Hivroz C, Fischer A, Korn H, Choquet D. The calcium current activated by T cell receptor and store depletion in human lymphocytes is absent in a primary immunodeficiency. *J Biol Chem* 1994; **269**:32327.

30 Alegre ML, Frauwirth KA, Thompson CB. T-cell regulation by CD28 and CTLA-4. *Nat Rev Immunol* 2001; **1**:220.

31 Chen L. Co-inhibitory molecules of the B7-CD28 family in the control of T-cell immunity. *Nat Rev Immunol* 2004; **4**:336.

32 Linsley PS, Greene JL, Brady W, Bajorath J, Ledbetter JA, Peach R. Human B7-1 (CD80) and B7-2 (CD86) bind with similar avidities but distinct kinetics to CD28 and CTLA-4 receptors. *Immunity* 1994; **1**:793.

33 Collins AV, Brodie DW, Gilbert RJ *et al.* The interaction properties of costimulatory molecules revisited. *Immunity* 2002; **17**:201.

34 van der Merwe PA, Bodian DL, Daenke S, Linsley P, Davis SJ. CD80 (B7-1) binds both CD28 and CTLA-4 with a low affinity and very fast kinetics. *J Exp Med* 1997; **185**:393.

35 Manzotti CN, Tipping H, Perry LC, Mead KI, Blair PJ, Zheng Y, Sansom DM. Inhibition of human T cell proliferation by CTLA-4 utilizes CD80 and requires $CD25^+$ regulatory T cells. *Eur J Immunol* 2002; **32**:2888.

36 Zheng Y, Manzotti CN, Liu M, Burke F, Mead KI, Sansom DM. CD86 and CD80 differentially modulate the suppressive function of human regulatory T cells. *J Immunol* 2004; **172**: 2778.

37 Pentcheva-Hoang T, Egen JG, Wojnoonski K, Allison JP. B7-1 and B7-2 selectively recruit CTLA-4 and CD28 to the immunological synapse. *Immunity* 2004; **21**:401.

38 Egen JG, Allison JP. Cytotoxic T lymphocyte antigen-4 accumulation in the immunological synapse is regulated by TCR signal strength. *Immunity* 2002; **16**:23.

39 Teh HS, Teh SJ. Direct evidence for a two-signal mechanism of cytotoxic T-lymphocyte activation. *Nature* 1980; **285**:163.

40 Fanger CM, Hoth M, Crabtree GR, Lewis RS. Characterization of T cell mutants with defects in capacitative calcium entry: genetic evidence for the physiological roles of CRAC channels. *J Cell Biol* 1995; **131**:655.

41 Bauer S, Adrian N, Williamson B *et al.* Targeted bioactivity of membrane-anchored TNF by an antibody-derived TNF fusion protein. *J Immunol* 2004; **172**:3930.

42 Thirion S, Motmans K, Heyligen H, Janssens J, Raus J, Vandevyver C. Mono- and bispecific single-chain antibody fragments for cancer therapy. *Eur J Cancer Prev* 1996; **5**:507.

43 Nicholson IC, Lenton KA, Little DJ, Decorso T, Lee FT, Scott AM, Zola H, Hohmann AW. Construction and characterisation of a functional CD19 specific single chain Fv fragment for immunotherapy of B lineage leukaemia and lymphoma. *Mol Immunol* 1997; **34**:1157.

44 Renner C, Jung W, Sahin U, van Lier R, Pfreundschuh M. The role of lymphocyte subsets and adhesion molecules in T cell-dependent cytotoxicity mediated by CD3 and CD28 bispecific monoclonal antibodies. *Eur J Immunol* 1995; **25**:2027.

45 Co MS, Avdalovic NM, Caron PC, Avdalovic MV, Scheinberg DA, Queen C. Chimeric and humanized antibodies with specificity for the CD33 antigen. *J Immunol*, 1992; **148**:1149.

46 Meissner P, Pick H, Kulangara A, Chatellard P, Friedrich K, Wurm FM. Transient gene expression: recombinant protein production with suspension-adapted HEK293-EBNA cells. *Biotechnol Bioeng* 2001; **75**:197.

47 Kipriyanov SM, Moldenhauer G, Little M. High level production of soluble single chain antibodies in small-scale *Escherichia coli* cultures. *J Immunol Methods* 1997; **200**:69.

48 Bauer S, Adrian N, Fischer E *et al.* Structure-activity profiles of Ab-derived TNF fusion proteins. *J Immunol* 2006; **177**:2423.

49 Renner C, Pfitzenmeier JP, Gerlach K, Held G, Ohnesorge S, Sahin U, Bauer S, Pfreundschuh M. RP1, a new member of the adenomatous polyposis coli-binding EB1-like gene family, is differentially expressed in activated T cells. *J Immunol* 1997; **159**:1276.

50 Quintana A, Schwarz EC, Schwindling C, Lipp P, Kaestner L, Hoth M. Sustained activity of calcium release-activated calcium channels requires translocation of mitochondria to the plasma membrane. *J Biol Chem* 2006; **281**:40302.

51 Quintana A, Schwindling C, Wenning AS, Becherer U, Rettig J, Schwarz EC, Hoth M. T cell activation requires mitochondrial translocation to the immunological synapse. *Proc Natl Acad Sci U S A* 2007; **104**:14418.

52 Challita-Eid PM, Penichet ML, Shin SU *et al.* A B7.1-antibody fusion protein retains antibody specificity and ability to activate via the T cell costimulatory pathway. *J Immunol* 1998; **160**:3419.

53 Peinelt C, Lis A, Beck A, Fleig A, Penner R. 2-Aminoethoxydiphenyl borate directly facilitates and indirectly inhibits STIM1-dependent gating of CRAC channels. *J Physiol* 2008; **586**:3061.

54 Prakriya M, Lewis RS. Potentiation and inhibition of Ca^{2+} release-activated Ca^{2+} channels by 2-aminoethyldiphenyl borate (2-APB) occurs independently of IP(3) receptors. *J Physiol* 2001; **536**:3.

55 Zang X, Allison JP. The B7 family and cancer therapy: costimulation and coinhibition. *Clin Cancer Res* 2007; **13**:5271.

56 Carlring J, Barr TA, Buckle AM, Heath AW. Anti-CD28 has a potent adjuvant effect on the antibody response to soluble antigens mediated through CTLA-4 by-pass. *Eur J Immunol* 2003; **33**:135.

57 Luhder F, Huang Y, Dennehy KM *et al.* Topological requirements and signaling properties of T cell-activating, anti-CD28 antibody superagonists. *J Exp Med* 2003; **197**:955.

58 Suntharalingam G, Perry MR, Ward S, Brett SJ, Castello-Cortes A, Brunner MD, Panoskaltsis N. Cytokine storm in a phase 1 trial of the anti-CD28 monoclonal antibody TGN1412. *N Engl J Med* 2006; **355**:1018.

59 Bluestone JA, St Clair EW, Turka LA. CTLA4Ig: bridging the basic immunology with clinical application. *Immunity* 2006; **24**:233.

Supporting Information

Additional Supporting Information may be found in the online version of this article:

Figure S1. Structural model of the antibodies and antibody fusion proteins are shown. All proteins were expressed with a C-terminal 6xHIS (grey) and myc (black) tag for IMAC purification and detection. The N-terminal orientation of the extracellular domain of CD80 and CD86 was chosen to assure appropriate receptor binding.

Figure S2. The binding properties of purified fusion proteins were analysed. Flow cytometric binding analysis of the indicated antibodies and antibody fusion proteins (10 μg/ml) on E6-1 Jurkat T-cells and CD33 expressing CHO cells.

Figure S3. Ca^{2+} signals depend on contact between T cells and CHO cells and on the presence of dscFv anti-CD33/anti-CD3.

Please note: Wiley-Blackwell are not responsible for the content or functionality of any supporting materials supplied by the authors. Any queries (other than missing material) should be directed to the corresponding author for the article.

